PCCP

ROYAL SOCIETY OF CHEMISTRY

PAPER

View Article Online
View Journal | View Issue

Cite this: *Phys. Chem. Chem. Phys.*, 2025, **27**, 10248

The integrity of the lipid bilayer structure is retained in natural occurring deep eutectic solvent water mixtures – a small angle X-ray scattering study

Marité Cárdenas, *[abc] Victoria Ariel Bjørnestad,[d] Kari Kristine Almåsvold Borgos[d] and Reidar Lund *[de]

Natural occurring deep eutectic solvents (NADES) are solvents made of metabolites occurring in living organisms, and are thought to play a special role in plants especially given that some of these metabolites exist in concentrations as high as 1 M. NADES have properties similar to ionic liquids, and have been shown to protect enzymes against loss of activity as well as proteins against thermal denaturation. Here, we explore the structure of lipid vesicles in NADES rich aqueous solutions and compare to concentrated saline aqueous solutions matching the various NADES osmolarity. The vesicle structure was analysed by small angle X-ray scattering (SAXS) and dynamic light scattering (DLS). Two types of NADES were prepared using choline chloride and glucose or maleic acid at a molar ratio of 1 : 1 giving the solvents a neutral or an acidic nature, respectively. The stability of the vesicles in the various solvents was measured against time and temperature. The results of this work demonstrate that lipid bilayers retain their structure in NADES rich aqueous solutions as compared to pure water, in contrast to high saline aqueous solutions. Moreover, the vesicles are more stable against sedimentation and aggregation in NADES than in water.

Received 24th January 2025,
Accepted 19th April 2025

DOI: 10.1039/d5cp00331h

rsc.li/pccp

Introduction

In recent years, deep eutectic solvents (DES) have been proposed as alternatives to organic solvents in a range of industrial applications[1] bringing great promise to achieve United Nations sustainable goals. DES share many properties with ionic liquids,[2] however they stand out by being made of a mixture of oppositely charged Lewis or Brønsted acids and bases. On their own, these are solids but form a liquid when mixed at given molar ratios.[1] Natural deep eutectic solvents (NADES) is the name given to DES formed by naturally occurring compounds, typically metabolites, that may exist in organisms such as plants and microorganisms at concentrations as high as 1 M.[3] DES and, particularly, NADES are superior with respect to ionic liquids as some of the latter are reported to be toxic and highly resistant to biodegradation.[4,5]

Given the high concentration of NADES components in nature, NADES were proposed as an alternative liquid phase (the third liquid phase in nature) with properties that are distinctive from the aqueous or lipid (oil) phase. In this way, specific compounds produced by plants can be stored and maintained in the plant at extremely high concentrations,[6] since their solubility in NADES can be hundreds of times higher than either in water or oil. Additionally, NADES have been proposed as a mechanism to protect the plant, and in particular its proteins, against external conditions such as extreme temperatures or low humidity:[7] enzyme stability upon storage in NADES rich aqueous solutions increased remarkably as compared to dilute water based buffers, even withstanding high temperature.[8] For example, plant enzymes were kept on the lab bench for weeks and fully recovered its function upon re-dilution in aqueous solution.[8]

The components in NADES typically include choline chloride and an acid such a maleic acid or citric acid, or a sugar such as glucose or glycerol.[3] Some of these compounds are expected to interact with amino acids or with the headgroups of phospholipids.[9] An all atom molecular dynamics (MD) simulation of choline chloride-based NADES on lipid bilayers

[a] *Department of Biomedical Science and Biofilm Research Center for Biointerfaces, Malmö University, 20506 Malmö, Sweden*
[b] *Instituto Biofisika (CSIC, UPV/EHU), Fundación Biofísica Bizkaia/Biofisika Bizkaia Fundazioa (FBB), 48940 Leioa, Spain. E-mail: marite.cardenas@ehu.eus*
[c] *Ikerbasque, Basque Foundation for Science, 48013 Bilbao, Spain*
[d] *Department of Chemistry, University of Oslo, Sem Sælandsvei 26, 0371 Oslo, Norway. E-mail: reidar.lund@kjemi.uio.no*
[e] *Hylleraas Centre for Quantum Molecular Sciences, University of Oslo, NO-0315 Oslo, Norway*

composed of 1-hexadecanoyl-2-(9*Z*-octadecenoyl)-*sn-glycero*-3-phosphocholine (POPC) suggested that hydrogen bonding moieties in NADES inserted in the headgroup region of the lipid bilayers without significantly affecting the lipid bilayer structure:[9] a change in the mean molecular area and thickness of at most 4.8% or −3% was calculated, respectively. The depth and extent of penetration in the bilayer structure (in terms of the number of NADES molecules in the bilayer as compared to the total number of molecules in the simulation box) increased with the hydrophobicity of the hydrogen donor molecule and ranged from 21% to 91% of available molecules for urea to phenylacetic acid, respectively. The less hydrophobic molecules stayed just below the phosphate groups of the phospholipids while those with greatest hydrophobicity reached the glycerol groups developing in some cases hydrogen bonding with these groups. Until date, there is no experimental report on the structure of lipid bilayers in NADES or NADES rich aqueous solutions, although the conservation of the vesicular structure was demonstrated by transmission electron microscopy (TEM) at up to 50 weight% NADES in water.[10] In the latter experiments though, osmolality was not kept constant across the vesicles upon NADES addition: vesicles were prepared in water and diluted in NADES which have osmolality matching M concentrations for simple salts.

On the other hand, it is not clear if NADES could form an adsorbed layer around the lipid bilayer in the presence of water which could serve as a potential mechanism to protect the bilayers under extreme conditions. The cryoprotection mechanism of trehalose, for example, was proposed to be the lowering of the gel to liquid crystalline phase transition temperature (T_m) at low water content so that the membrane structure is retained during drying and rehydration.[11] Trehalose is supposed to intercalate in the phospholipid headgroups creating new hydrogen bonding that substitutes those with water.[12] An atomistic MD simulation on lipase structure and solvation in NADES, 50% NADES in water and water showed that dilution of NADES in water does not displace NADES molecules from the aqueous solvation shell around the lipase but rather H_2O molecules incorporate within the space in between the bulkier NADES molecules increasing the total number of hydrogen bonding within the solvation shell.[13]

In this paper, we aimed to produce vesicles in NADES rich aqueous solutions by the extrusion method and to characterise the effect of NADES on their structure by means of small angle X-ray scattering (SAXS). Two types of NADES were used: (1) an equimolar mixture of choline chloride (Ch) and glucose (G) that gives an overall neutral charge to the solvent, and (2) an equimolar mixture of Ch and maleic acid (M) that gives a negative charge to this solvent (balanced by the counterion). Vesicles were prepared from zwitterionic POPC and also including 20 mol% of 1-hexadecanoyl-2-(9*Z*-octadecenoyl)-*sn-glycero*-3-phospho-(1′*rac* glycerol) (sodium salt) (POPG) to give a negative charge to the vesicles. Vesicles were prepared in 0–75 wt% NADES, under biologically relevant conditions that match the study by Knudsen *et al.*[8] on membrane bound enzyme activity in NADES rich *versus* poor aqueous solutions. Preparing vesicles by extrusion in pure NADES was not possible due to the known high viscosity characteristic of these solvents. Even though it is – from a pure physical chemical angle – interesting to look at NADES alone, the results will not be relevant to the biological conditions we are looking after to mimic in this study. Fig. 1 gives the chemical structure of NADES and lipids used in this work.

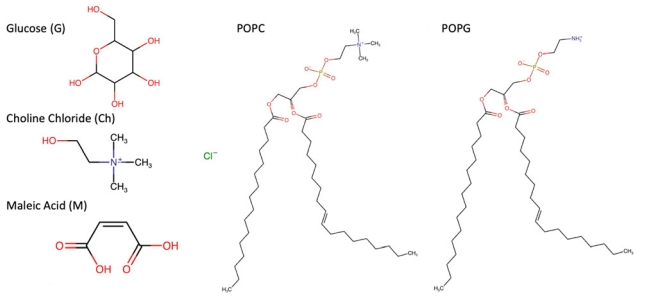

Fig. 1 The chemical structure of the components of NADES: glucose, choline chloride, and maleic acid, and the phospholipids POPC and POPG.

Experimental

Materials

Maleic acid (Thermo Scientific, purity ≥ 98%), choline chloride (Thermo Scientific, purity 99%), glucose (Sigma, purity ≥ 99.5%), NaCl (Sigma, purity ≥ 99%), POPC and POPG (Avanti Lipids, purity ≥ 99%) were used as purchased. MilliQ water was used for all experiments.

NADES preparation

NADES of choline and glucose (neutral NADES) and choline and maleic acid (acidic NADES) were prepared as equimolar mixtures as follows:

Choline chloride and glucose (ChG) NADES

12.9040 g of glucose was weighed out and dissolved in 40.0044 g of water. The solution was heated and sonicated to quickly *e.g.* dissolve clumps of sugar. 10.0002 g of choline chloride was weighed out and dissolved in 40.0091 g of water. The two components were then mixed in a round-bottom flask and each flask was rinsed with 2 mL water, giving a total of ∼84 mL of water in the solution. The flask was then placed on the rotary evaporator in a water bath of 45 °C at 70 mbar to evaporate overnight all non-bound water. The initial water content was thus 800 135. After evaporating the water the final sample weight was 103.307 g. This means that at least 91% of the original water was removed. Later measurement found that the average water content from triplicate measurements of the sample was 1.2 wt%. 75, 50 and 25 wt% NADES solutions were prepared from the stock by dilution with water.

To make NaCl solutions with corresponding ionic strength, 3.57 M and 1.79 M solutions of NaCl were prepared to match the 50 and 25 wt% NADES, respectively. The 75% was not

matched with NaCl solution since NaCl is very close to its solubility point at this concentration.

Choline chloride and maleic acid (ChM) NADES

8.3137 g of maleic acid was weighed out and dissolved in 40.0421 g of water. 10.0001 g of choline chloride was weighed out and dissolved in 40.0091 g of water. The two components were then mixed into a round-bottom flask and each flask was rinsed with 2.5 mL of water, giving a total of ~84 mL of water in the solution. The flask was then placed on the rotary evaporator in a water bath of 45 °C at 70 mbar to evaporate overnight. The final weight after water evaporation was 102.3039 g, meaning at least 96% of the original water was removed. Later measurement found that the average water content from triplicate measurements of the sample was 4.7 wt%. 50 and 25% NADES solutions were prepared from the stock by dilution with water.

NADES characterisation

Density measurements were performed using the DMA 5000 density meter from Anton Paar. From the separate measurement of the solution (NADES and lipid vesicle) and solvent (NADES), the specific volume was calculated according to:

$$v_s = \left(\frac{1}{c_{sol}}\right) \cdot \left(\frac{1}{d_{sol}}\right) - \left(\frac{1 - c_{sol}}{c_{sol}}\right) \cdot \left(\frac{1}{d_0}\right) \quad (1)$$

Where c_{sol} is the weight fraction of the lipids, d_{sol} and d_0 are the densities of the lipid solution and solvent respectively.

Refractive index was measured using the NAR-1T Abbe Refractometer using a wavelength of 589.3 nm. Measurements were done in triplicates and values reported are accurate to ±1%.

Viscosity was measured with the Rheometer Bohlin CVO 100 Digital equipped with Peltier Cylinder C25 using a cone 4/40 system at a shear rate of 0.125. Measurements were taken in triplicates and values reported are accurate to ±2%.

Lipid vesicle preparation

Lipid vesicles were prepared by weighing out an appropriate amount of POPC/POPC and POPG powder into a round-bottom flask and dissolving in a 3:1 mixture of chloroform and methanol. For the POPC–POPG samples, the weight was calculated to give 20 mol% POPG in the lipid mixture. A dry lipid film was then produced by evaporating the organic solvent under a flow of nitrogen gas and then leaving it under vacuum for at least one hour (samples for DLS experiments) or overnight at 70 mbar in waterbath at 45 °C (samples for SAXS experiments). An appropriate volume of either (1) NADES solution, (2) water and/or (3) NaCl solution was added to the film to give a final concentration of 10 mg mL^{-1}. The solutions were then bath sonicated for 20 minutes before they were extruded 3 times at 25 °C through 100 nm filters. Earlier studies have shown that 2 passages through the extruder suffice to get a good polydispersity.[14,15] The measured physical chemical parameters are listed in Table 1.

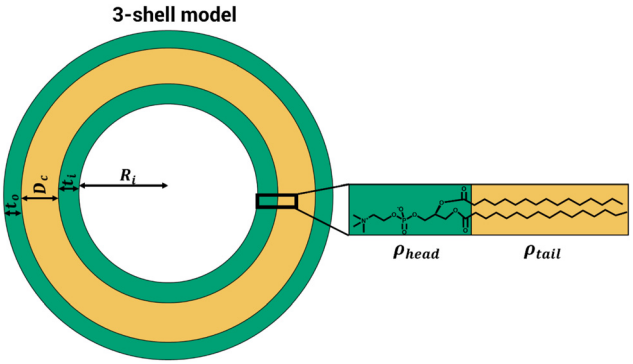

Fig. 2 Illustration of the 3-shell model. t_o = thickness of outer head shell, D_c = thickness of tail shell, t_i = thickness of inner head shell, R_i = inner radius, ρ_{head} = SLD headgroup and ρ_{tail} = SLD tailgroup. The interfaces between the shells as described by the interfacial width, σ_i.

Small angle X-ray scattering (SAXS)

Measurements. All measurements were performed using a Bruker Nanostar SAXS instrument at the Norwegian centre for X-ray diffraction and the scattering and imaging REsource centre X-rays (RECX). The data were obtained using a wavelength of 1.54 Å and a detector distance of 1.07 m, covering a Q range of about 0.009 to 0.29 Å^{-1}. The solutions were injected into the capillary shortly after mixing (~1 hour) and then several SAXS measurements were made consecutively to test the stability over time. For each measurement, the background of the corresponding solvent was measured before the sample measurement.

Data modelling. The SAXS measurements of the POPC and DPPC vesicle were analysed using the 3-shell model which was found to describe the data well with minimum number of parameters. The model is illustrated in Fig. 2, where 1 shell accounts for the hydrocarbon region of the bilayer and 2 surrounding shells account for the headgroup regions on the

Table 1 Physicochemical parameters for neutral (ChG) and acidic (ChM) NADES

	NADES (%vol)	NADES (%mol)	Viscosity (Pa s)	Refractive index	Density (g L^{-1})	Water[a] (%wt)
ChM	5	0.5	0.0418	1.339	1.30	4.7
	30	3.8	0.0594	—		
	50	8.4	0.0627	1.409		
	94	59	0.6321	1.482		
ChG	5	0.4	0.0652	1.339	1.28	1.2
	15	1.3	0.0555	1.352	1.30	
	50	6.8	0.0738	1.405	1.30	
	89	37.2	0.1489	1.469	1.31	

[a] For pure (100%) NADES.

outer and inner leaflet. The scattering amplitude is expressed as the sum of the form factors of 3 concentric shells:

$$A(Q)_{3\text{-shell}} = \sum_{i=1}^{i=3} \Delta\rho_i \cdot V_i \cdot A(Q, R_i, R_{i-1})_{\text{shell}} \quad (2)$$

where V_i are the different shell volume:

$$V_i = \frac{4\pi}{3}\left(R_i^3 - R_{i-1}{}^3\right) \quad (3)$$

and $\Delta\rho_i$ is the contrast of that respective shell, defined as $\Delta\rho_i = \rho_i - \rho_0$, where ρ_0 is the scattering length density (SLD) of the solvent (in this case either NADES, water or NaCl-solution) and ρ_i the SLD of the respective shell. The SLD of the solvent is calculated based on the number of electrons in the solute molecule, its molecular mass and measured density. The values are summarized in Table 2. The SLD for the hydrocarbon region is calculated from the number of electrons, Z_{tail}, and the volume of a single lipid tail, V_{tail}:

$$\rho_{\text{HC}} = \frac{Z_{\text{tail}}}{V_{\text{tail}}} \cdot r_0 \quad (4)$$

with r_0 being the Thompson scattering length. In the headgroup shells, the hydration is also considered when calculating the SLDs. The SLD for a particular shell i = inner|outer is:

$$\rho_i = (1 - f_{\text{w,outer}}) \cdot \rho_{\text{head}} + f_{\text{w,i}} \cdot \rho_0 \quad (5)$$

And the parameter $f_{\text{w,i}}$ is the calculated fraction of water in that shell:

$$f_{\text{w,i}} = 1 - \frac{V_{\text{head}} \cdot P_{\text{agg}} \cdot 0.5}{V_i} \quad (6)$$

where the aggregation number P_{agg} is calculated from the how many lipid tail groups of volume V_{tail} fit into the tail group shell V_{c} calculated as in eqn (3):

$$P_{\text{agg}} = \frac{V_{\text{c}}}{V_{\text{tail}}} \quad (7)$$

When using a common shell for the hydrophobic group, we need to make an assumption about the aggregation number in the outer and inner leaflet to calculate the hydration of the headgroup shells. Here, we have used the simplification that half of the lipids are in each leaflet; one might want to try other assumptions, however, we have found that the difference in the fits (tested by the exact calculation using of two shells from the hydrocarbon region as described in the next section) is completely insignificant in our fits. The headgroup SLD is calculated in the same way as it was for the acyl tail group:

$$\rho_{\text{head}} = \frac{Z_{\text{head}}}{V_{\text{head}}} \cdot r_0 \quad (8)$$

The scattering amplitude for each shell is defined as:

$$A(Q)_{\text{shell}} = \frac{\frac{4\pi R_i^3}{3} \cdot A(Q, R_i)_{\text{sphere}} \cdot \exp\left(-\frac{Q^2\sigma_i^2}{2}\right) - \frac{4\pi R_{i-1}{}^3}{3} \cdot A(Q, R_{i-1})_{\text{sphere}} \cdot \exp\left(-\frac{Q^2\sigma_{i-1}{}^2}{2}\right)}{V_{i-1}} \quad (9)$$

where R_i and R_{i-1} represent the outer and inner radii of the shell, while σ_i and σ_{i-1} are the disorder parameters for the inner and outer boundaries of the shell. $A(Q,r)_{\text{sphere}}$ is the spherical form factor and is defined as:

$$A(Q, r)_{\text{sphere}} = \frac{3 \cdot (\sin(Q \cdot r) - Q \cdot r \cdot \cos(Q \cdot r))}{(Q \cdot r)^3} \quad (10)$$

To account for the multilamellarity of the liposomes, we used the modified Caillé theory structure factor:[16]

$$S_{N_k,\text{MC}} = N_{\text{diff}} + N_k + 2 \cdot \sum_{k-1}^{N_k-1} (N_k - k)\cos(kQd) \times \exp\left(\left(-\frac{d}{2\pi}\right)Q^2\eta_1\gamma\right)(nk)^{\left(\frac{d}{2\pi}\right)^2 Q^2\eta_1} \quad (11)$$

where N is the average number of bilayers in the multilamellar structure, N_{diff} is the number of uncorrelated scattering bilayers, d is the mean stacking separation, γ is the Euler's constant and η_1 is the Caillé parameter which accounts for the bilayer fluctuations. The final structure factor becomes:

$$S_{\text{MC}}(Q,N_k) = (1 - w)S_{[N_k],\text{MC}}(Q) + wS_{[N_k]+1,\text{MC}}(Q) \quad (12)$$

where $w = N_k - [N_k]$.

To account for polydispersity in the size of the different stacks, we use an average over a Gaussian distribution where σ is the standard deviation of the Gaussian-weighted distribution, making:

$$S(Q) = \sum_{N_k-N-2\sigma}^{N_k+2\sigma} x_k(N_k)S_{\text{MC}}(Q, N_k) \quad (13)$$

where

$$x_k = \frac{1}{\sigma\sqrt{2\pi}}\exp\left(-\frac{(N_k - N)^2}{2\sigma^2}\right) \quad (14)$$

The final scattering intensity is then calculated as:

$$\langle I(Q)\rangle = \left[\frac{\phi}{\langle V\rangle}\int_0^\infty f(R_{\text{tot}}) \cdot A(Q)_{3\text{-shell}} \cdot A(Q)_{3\text{-shell}}\mathrm{d}r\right] \times (f_{\text{uni}} + (1 - f_{\text{uni}}) \cdot S(Q)) \quad (15)$$

Note that this expression using a decoupling between form and structure factor, implicitly neglect curvature. It is thus valid

Table 2 Measured densities for neutral (ChG) and acidic (ChM) NADES, and the corresponding X-ray SLDs of the solutions

	%NADES (% mass)	Density (g L^{-1})	SLD (cm^{-2})
Water	0	0.998	9.40×10^{10}
ChG	0.25	1.056	9.69×10^{10}
	0.5	1.134	1.04×10^{11}
	0.75	1.211	1.11×10^{11}
ChM	0.25	1.057	9.61×10^{10}
	0.5	1.094	9.90×10^{10}

for locally flat bilayer as is the case for the separated scattering form factor (SFF) which can be used describe more detailed structural features within a bilayer.[17–19] A formalism showing the the separation of structure and form factor for MLVs has been presented by Frielinghaus.[20] The fit model was implemented as C++ code in the qtiSAS developed by Dr Vitaliy Pipich.[21]

Electron density profiles

Based on the structural parameters obtained by the three-shell model, volume fractions of lipids in the different shells were determined and the electron density profiles of the bilayer was calculated by scaling the volume fractions of the convolved density blocks with their SLDs.

Dynamic light scattering (DLS)

DLS was measured using a Nanosizer from Malvern. The correlation functions were fitted using

$$g_2(t) - 1 = A \exp\left[-\left(\frac{1}{\tau}\right)^{\beta}\right]$$

where β is close to 1.

Where the diameter, D, was calculated using the Stokes–Einstein equation as follows

$$D = \frac{\tau k_B T}{3\pi\eta \cdot Q^2}$$

where η is the viscosity, Q is the momentum of the momentum transfer vector for the DLS measurement, k_B is the Boltzman constant, and T is the temperature. Triplicate measurements were made.

Results and discussions

Vesicles in choline chloride and glucose (ChG) NADES aqueous solutions

SAXS data was collected for the two different vesicle compositions (POPC *vs.* POPC:POPG) resuspended in water, 3.57 M NaCl solution or in ChG NADES rich aqueous solutions, and representative data is shown in Fig. 3 and 4 for POPC and POPC–POPG vesicles, respectively. The saline conditions used match the osmolarity of the NADES used (specifically 1.79 M NaCl and 3.57 M NaCl match 25% and 75% NADES respectively). Not much information can be extracted qualitatively from the data because of the major changes in contrast upon changing the solvent from pure water to 75% NADES. However, multilamellar structures clearly exist for POPC vesicles (Fig. 3), as shown by the Bragg peaks occurring at $Q \approx 0.1$ regardless of the solvent. The degree of multi lamellarity though, which is reflected in the shape of the Bragg peak: *i.e.*, its intensity and sharpness, depended on the solution used. First, the Q position of the Bragg peak slightly shifted to higher Q for ChG NADES rich aqueous solutions with respect to both pure water and NaCl solution. This Bragg peak relates to the lamellar repeat distance (lipid bilayer thickness + the solvent layer thickness in between bilayers). Thus, the interlamellar distance became smaller in NADES rich solutions compared to water and NaCl aqueous solution (Table 3). Moreover, the Bragg peak in 50 wt% ChG NADES was broader than in water suggesting a more disorganised structure. As proposed by MD simulations,[15,16] the molecules forming NADES could penetrate the headgroup region substituting water for hydrogen bonding. Such penetration could increase the apparent vesicle charge altering not only the lamellar repeat distance but also the extent of multi

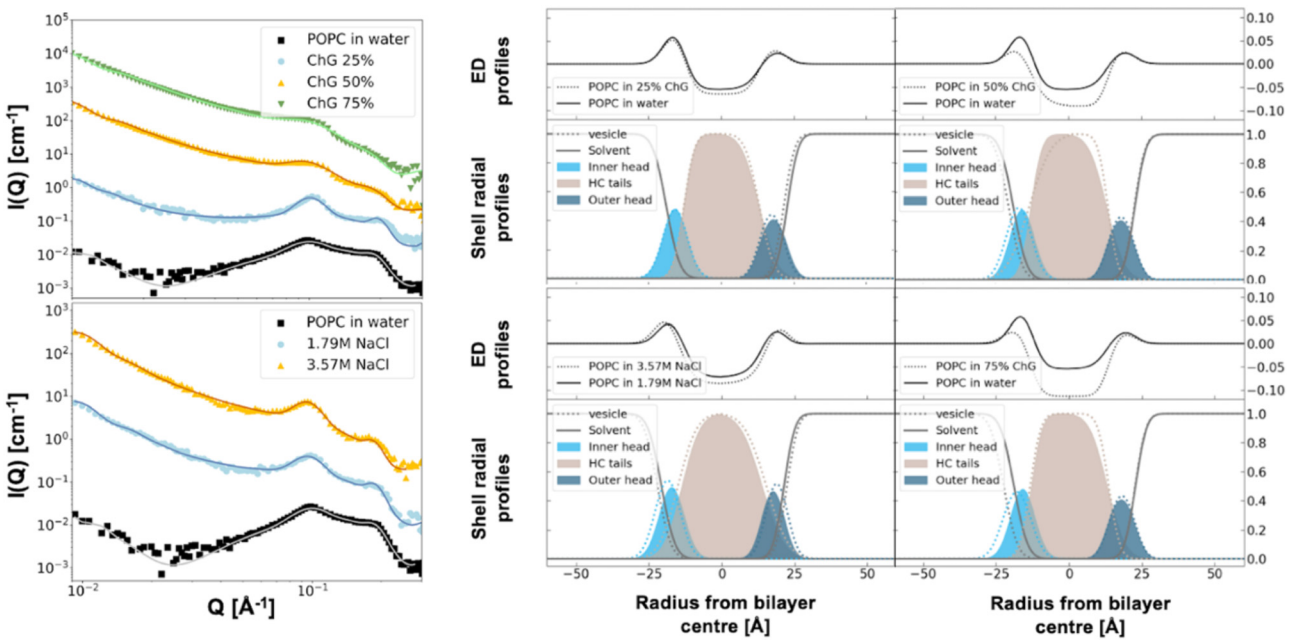

Fig. 3 SAXS (scaled) scattering patterns for POPC vesicles in the different solvent: water, 3.57 M NaCl, 25, 50 and 50 wt% choline chloride: glucose NADES in water. Electron density (ED) profiles and shell radial profiles corresponding to the best fits are shown to the right.

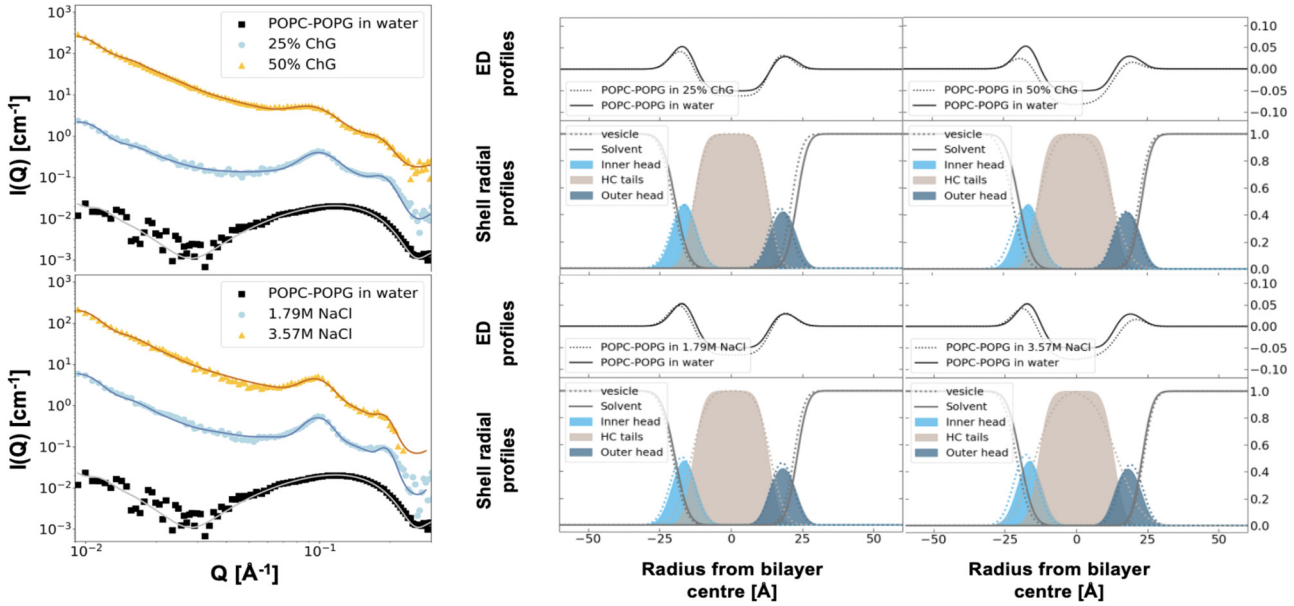

Fig. 4 SAXS (scaled) scattering patterns for POPC–POPG vesicles in the different solvent: water, 3.57 M NaCl, 25, 50 and 50 wt% choline chloride: glucose NADES in water. Electron density (ED) profiles and shell radial profiles corresponding to the best fits are also shown.

lamellarity. Note that the consecutive increase in NADES concentration first induced an increase and then a decrease in multi-lamellarity for POPC (67, 43, 65 and 65% unilamellar vesicles in 0, 25, 50 and 75% ChG NADES respectively, Table 3). The extent of multi-lamellarity has been proposed to depend on the vesicle surface charge and the bilayer's bending rigidity. A possible explanation for this behaviour consists in the increasing number of NADES molecules that could penetrate the headgroup region of the bilayer as the NADES concentration increases,[22,23] first leading to an increase in the apparent vesicle surface charge and then a lowering of their bending rigidity which would counteract the surface charge effect. Ionic liquids have been shown to modulate the bending rigidity of membranes, with the net effect depending on the type of ionic liquid and the lipid itself.[24]

For the charged vesicles (POPC–POPG, Fig. 4), unilamellarity was observed in pure water. This is probably due to the inter vesicle electrostatic repulsion from the added POPG lipids, an effect that is well known from the literature.[26] However, the negative charges in POPG are efficiently screened in the presence of either NaCl or NADES resulting in the reappearance of the Bragg peaks seen in the scattering profile for uncharged POPC vesicles. In the charged vesicle system, the shift in Q was less obvious which suggests similar interlamellar spacing in NADES and NaCl aqueous solutions (Table 3). However, the peak was less sharp in NADES compared to NaCl similarly to

Table 3 Model parameters obtained for the best fits of the 3-shell model to the SAXS dats for POPC vesicles in different solutions shown in Fig. 3

Parameter	Water	1.79 M NaCl	3.57 M NaCl	25% ChG	50% ChG	75% ChG
Inner radius (Å)	600 ± 150	400 ± 33	380 ± 33	680 ± 30	404 ± 30	397 ± 30
Thickness inner headgroup shell (Å)	6.0 ± 0.6	7.0 ± 2.5	7.0 ± 2.5	6.0 ± 1.5	7.0 ± 1.5	9.0 ± 1.5
Thickness outer headgroup shell (Å)	9.7 ± 0.7	7.5 ± 2.0	7.0 ± 2	8.5 ± 2.5	9.0 ± 2.5	9.0 ± 2.5
Thickness tail shell (Å)	13.0 ± 0.4	13.8 ± 0.8	15.2 ± 0.8	13.0 ± 0.4	13.5 ± 0.4	13.5 ± 0.4
$\sigma_{\text{inner tail}}$ (Å)	3.0 ± 0.6	5.0 ± 2.1	5.2 ± 2.1	3.9 ± 0.7	6.0 ± 0.7	3.0 ± 0.7
$\sigma_{\text{outer tail}}$ (Å)	4.9 ± 0.5	6.0 ± 1.3	6 ± 1.3	3.7 ± 1.4	2.8 ± 1.4	3.0 ± 1.4
$\sigma_{\text{inner head}}$ (Å)	3.7 ± 0.9	3.7 ± 2	3.7 ± 2	3.7 ± 1.9	3.7 ± 1.9	3.7 ± 1.9
$\sigma_{\text{outer head}}$ (Å)	3.0 ± 1.7	3.0 ± 2	3.0 ± 2	3.0 ± 2.5	3.0 ± 2.5	3.0 ± 2.5
Volume headgroup[a] (Å^3)	331	331	331	331	331	331
Volume total lipid (Å^3)	1248 ± 3	1278 ± 4	1291 ± 4	1248 ± 3	1249 ± 3	1244 ± 3
Fraction of water in inner headgroup shell[b]	0.176	0.25	0.176	0.176	0.245	0.406
Fraction of water in outer headgroup shell[b]	0.543	0.41	0.316	0.543	0.502	0.50
Fraction of unilamellar vesicles	0.67 ± 0.03	0.46 ± 0.05	0.53 ± 0.05	0.43 ± 0.02	0.61 ± 0.02	0.65 ± 0.02
Fraction of unilamellar vesicles[c]	0.71 ± 0.03	0.56 ± 0.05	0.48 ± 0.05	0.37 ± 0.02	0.65 ± 0.02	0.62 ± 0.02
Number of layers in the multilamellar vesicles	2.4 ± 0.2	2.7 ± 0.3	3.0 ± 0.3	3.0 ± 0.2	2.5 ± 0.2	2.3 ± 0.2
σ_d (Å)	3.8 ± 1.7	4 ± 3	5 ± 3	4.0 ± 1.6	7.9 ± 1.6	9.0 ± 1.6
Repeating distance (Å)	64.7 ± 0.8	64.7 ± 1.6	64.7 ± 1.6	61.0 ± 1.3	61.9 ± 1.3	60 ± 1.3
Background	0.0011	0.001	0.0022	0.002	0.002	0.0022
σ_{PD} SD	0.14	0.20	0.22	0.13	0.22	0.2

[a] Fixed parameters as reported by literature values.[25] [b] Indicate parameters as calculated in the model. [c] When N held at 2.5.

Table 4 Model parameters obtained for fits of the three-shell model to the SAXS data for 80%POPC–20%POPG vesicles in different solutions shown in Fig. 4

Solvent	Water	1.79 M NaCl	3.57 M NaCl	25% ChG	50% ChG
Inner radius (Å)	600 ± 92	398 ± 41	402 ± 41	391 ± 33	380 ± 33
Thickness inner headgroup shell (Å)	6.6 ± 2.5	6.5 ± 2.6	6.5 ± 2.6	7.5 ± 2.1	9.0 ± 2.1
Thickness outer headgroup shell (Å)	9.7 ± 2.0	8.0 ± 2.7	9.0 ± 2.7	8.0 ± 2.1	9.0 ± 2.1
Thickness tail shell (Å)	13.2 ± 0.6	13.9 ± 0.5	14.5 ± 0.5	13.1 ± 0.5	13.0 ± 0.5
$\sigma_{\text{inner tail}}$ (Å)	3.0 ± 1.1	4.4 ± 1.7	5.6 ± 1.7	3.5 ± 1.6	4.2 ± 1.6
$\sigma_{\text{outer tail}}$ (Å)	3.0 ± 1.4	4.0 ± 2.0	6.7 ± 2.0	3.0 ± 1.8	4.9 ± 1.8
$\sigma_{\text{inner head}}$ (Å)	3.7 ± 2.2	3.7 ± 2.4	3.7 ± 2.4	3.7 ± 2.0	3.7 ± 2.0
$\sigma_{\text{outer head}}$ (Å)	3.0 ± 2.5	3.0 ± 2.3	3.0 ± 2.3	3.0 ± 2.1	3.0 ± 2.1
Volume headgroup[a] (Å^3)	331	331	331	331	331
Volume total lipid (Å^3)	1236 ± 2	1262 ± 2	1263 ± 2	1241 ± 2	1226 ± 2
Fraction of water in inner headgroup shell[b]	0.22	0.17	0.137	0.310	0.418
Fraction of water in outer headgroup shell[b]	0.53	0.43	0.476	0.451	0.509
Fraction of unilamellar vesicles	1 ± 0.01	0.46 ± 0.05	0.55 ± 0.05	0.51 ± 0.05	0.61 ± 0.05
Fraction of unilamellar vesicles[c]	NA	0.45 ± 0.05	0.55 ± 0.05	0.51 ± 0.05	0.65 ± 0.05
Number of layers in the multilamellar vesicles	NA	2.9 ± 0.3	2.5 ± 0.3	2.5 ± 0.1	2.2 ± 0.1
Sigma_d (Å)	NA	3.0 ± 2.5	3.8 ± 2.5	6.0 ± 2.5	6.9 ± 2.5
Repeating distance (Å)	NA	63.0 ± 1.5	63.5 ± 1.5	62.8 ± 1.4	64.0 ± 1.4
Background	0.0011	0.0007	0.0007	0.001	0.0011
Sigma_Gauss_SD	0.20	0.17	0.2	0.2	0.22

[a] Fixed parameters as reported by literature values.[25] [b] Indicate parameters as calculated in the model. [c] When N held at 2.5.

the uncharged vesicle system. The same trend as for POPC was observed where the degree of multi-lamellarity first increased and then decreased upon increasing the NADES concentration (Table 3).

The SAXS data were analysed with a three-shell vesicle model with a paracrystalline structure factor to account for the multi-lamellarity. The best fits to the parameters listed in Tables 3 and 4 for POPC and POPC–POPG vesicles are displayed as lines in Fig. 3 and 4, respectively. The fits did not reveal any major structural changes in the lipid bilayer as the solvent is transitioned from pure water to containing 75 wt% NADES. The main changes occurred around the headgroup region, as expected, with the inner headgroup layer thickness increasing drastically at the highest NADES concentration in water. Note that the structural changes in the lipid bilayer in NADES differ significantly from those in saline water-based solutions. When NaCl was added, a 2.2–2.3 Å increase in the tail thickness took place as compared to pure water. The head group thickness, instead, remained roughly unchanged despite the significant dehydration of the headgroup. Moreover, an increase in the tail volume occurred in saline conditions while no change in tail volume was observed in NADES rich aqueous solutions. The effect seen in saline conditions (increase in both lipid volume and tail thickness) is opposite to what is seen for example during melting from the gel to the fluid phase;[27] the lipid area increased slightly in the NaCl solutions, but much less than upon melting. The volume change is thereby not due to lateral expansion of the lipid in the bilayer in saline conditions. Thus, we can conclude that the presence of the NADES moieties protects the bilayer against major structural changes due to high osmolarity.

An attempt was also made at fitting the data to a model which incorporated the possibility to have an excess of NADES in the headgroup region. This implies that the hydration layer of the vesicles could contain more NADES than the bulk solvent. However, when freeing the parameter adjusting the excess NADES in the hydration layer, the fit would consistently fit to zero or approximately zero, so excess NADES in the hydration of the headgroup does not explain the small deviations in the 3-shell model from the experimental data. Attempts at "forcing" NADES into the hydration layer just caused the fit to go towards dehydration of the headgroups. One option could, of course, be that only one of the components is interacting with the bilayer, but this makes it difficult to know anything about the density of the solution around the headgroup and would be equivalent to just fitting the hydration SLD to an arbitrary value within range of the values for water and NADES, and seemingly would be better studies by other methods such as the combination of selective deuteration and small angle neutron scattering.[28] This is consistent with atomistic MD simulations that suggest that upon diluting pure NADES to 50% in water, the water molecules would not replace NADES for

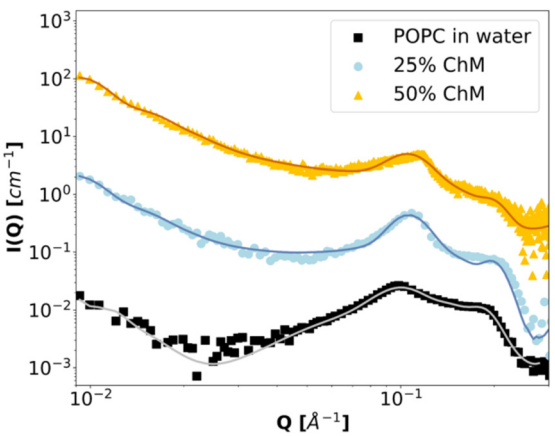

Fig. 5 SAXS data with model fits of the three-shell model with POPC vesicles in different solutions of ChM-NADES. The intensities are scaled by factors of ten.

hydrogen bonding with a lipase, but instead fill in the empty space in between the bulkier NADES molecules.[19] A five-shell model, with an inner and outer shell to include a surplus of NADES in between the tail and head group shells, was also attempted without accounting for any further deviations from the original three-shell fit, despite this model being able to induce more drastic changes in the SAXS curve.

Finally, the vesicle size decreased as a function of either salt or NADES concentration (Tables 3 and 4). Dynamic light scattering (DLS) data was collected (Fig. 6) to corroborate the SAXS results in terms of the trends in the overall size of the vesicles. The hydrodynamic-based vesicle diameter decreased down to roughly 25 nm with NADES concentration, reaching a plateau at 30% NADES. The same effects were observed regardless of lipid composition in the vesicles, or the type of NADES used.

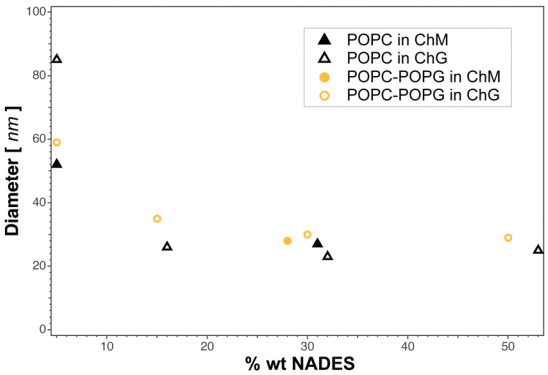

Fig. 6 Dynamic light scattering data for vesicles as a function of NADES concentration in water.

Vesicles in choline chloride and maleic acid (ChM) NADES aqueous solutions

POPC vesicles were also prepared in 25 and 50% acidic ChM NADES and SAXS data collected as shown in Fig. 5. The best fit to the three-layer vesicle model (Table 4 lists the parameters used in the best fits shown in Fig. 5) demonstrate that no significant changes in the bilayer structure took place for this NADES composition either. The extent of multi-lamellarity though was lower as compared to neutral NADES (Fig. 3). This effect could be due to the integration of the NADES pairs in the headgroup region as suggested by MD simulations,[18] which would give a higher apparent negative charge to the vesicles and thus decrease multi-lamellarity (Table 5).[26]

The retained lipid bilayer structure in high NADES concentration suggests that the effects in decreased enzymatic activity for membrane bound enzymes in high NADES concentration in water[8] is not due to changes in the lipid bilayer structure that could affect the lipid–protein interface. Rather such membrane bound enzyme activity modulation likely arises from NADES–protein interactions as, for example, the replacement of water from the solvation shell of the enzyme's active site.[22]

Stability in time and towards temperature

Finally, the vesicles prepared in NADES containing aqueous solutions were stored over time (up to 11 hours) at room temperature and also at 37 °C, and the SAXS profile was collected over time (Fig. 7). For comparison, vesicles prepared in pure water or in saline conditions were also measured. There seem to be small differences over time especially for the charged vesicle system as expected, therefore the data was replotted as $(I - I_o)/(I + I_o)$ *vs.* Q in Fig. 8. Some deviations occur around the Q position where the Bragg peak appears for water only. The stability over time also increases with NADES concentration with non-observable changes seen for 75% NADES in water. In terms of temperature, larger differences in the SAXS signal take occur at low Q for H_2O as compared to NADES containing solutions. This would imply that the vesicles are subjected to larger structural changes in terms of the vesicle size due to temperature in water than when NADES is present

Table 5 Model parameters obtained for best fits of the three-shell model to POPC vesicles SAXS data in ChM NADES containing aqeuous solutions shown in Fig. 5

	Water	25% ChM	50% ChM
Inner radius (Å)	600 ± 150	400 ± 75	400 ± 75
Thickness inner headgroup shell (Å)	6.0 ± 0.6	6.0 ± 1.1	6.0 ± 1.1
Thickness outer headgroup shell (Å)	9.7 ± 0.7	9.7 ± 1.9	9.7 ± 1.9
Thickness tail shell (Å)	13.0 ± 0.3	13.2 ± 0.5	13.2 ± 0.5
$\sigma_{\text{inner tail}}$ (Å)	3.0 ± 0.6	6.0 ± 0.6	3.0 ± 0.6
$\sigma_{\text{outer tail}}$ (Å)	4.9 ± 0.4	3.5 ± 1.3	5.1 ± 1.3
$\sigma_{\text{inner head}}$ (Å)	3.7 ± 0.9	3.7 ± 1.3	3.7 ± 1.3
$\sigma_{\text{outer head}}$ (Å)	3.0 ± 1.7	3.0 ± 1.7	3.0 ± 1.3
Volume headgroup[a] (Å^3)	331	331	331
Volume total lipid (Å^3)	1248 ± 2	1253 ± 3	1253 ± 3
Fraction of water in inner headgroup shell[b]	0.176	0.145	0.145
Fraction of water in outer headgroup shell[b]	0.543	0.551	0.551
Fraction of unilamellar vesicles	0.67 ± 0.03	0.28 ± 0.08	0.53 ± 0.08
Number of layers in the multilamellar vesicles	2.4 ± 0.2	3.0 ± 0.2	2.6 ± 0.2
Sigma_d (Å)	3.8 ± 1.7	5.0 ± 1.9	5.0 ± 1.9
Repeating distance (Å)	64.7 ± 0.8	58.6 ± 0.6	57.8 ± 0.6
Background	0.0011	0.0003	0.00025
Sigma_Gauss_SD	0.14	0.22	0.2

[a] Indicate parameters fixed as reported by literature values.[25] [b] Indicate parameters as calculated in the model.

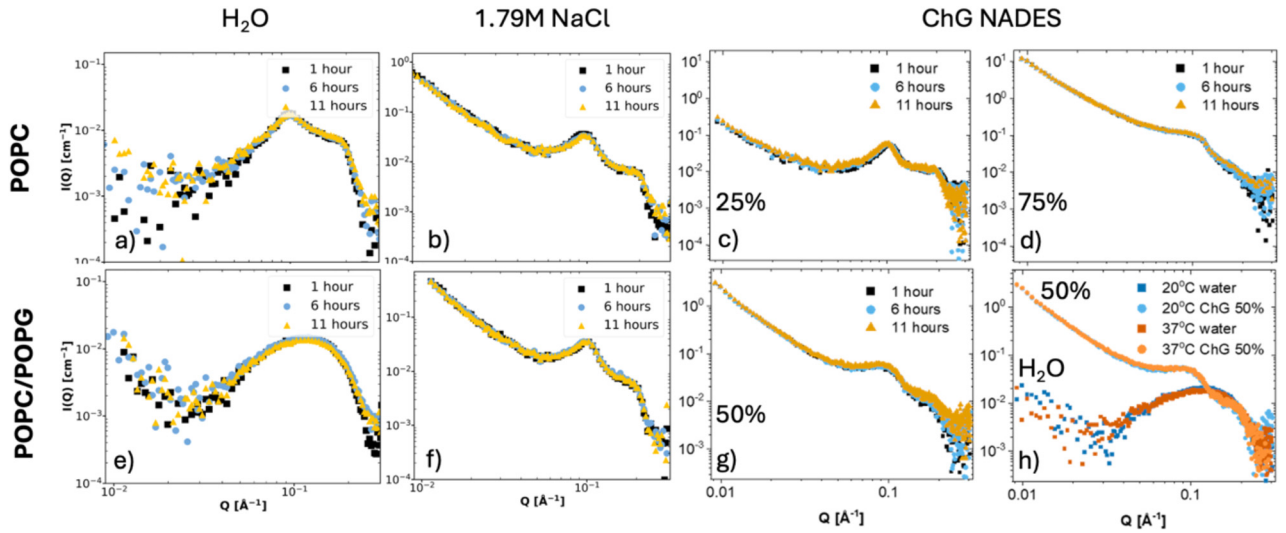

Fig. 7 SAXS curves for POPC vesicles in (a) water, (b) 1.79 M NaCl, (c) 25% ChG NADES and (d) 75% ChG NADES and POPC–POPG (bottom row) measured over time from preparation at 1, 6 and 11 hours. The bottom row shows SAXS curves for POPC/POPG vesicles in (e) water, (f) 1.79 M NaCl, (g) 50% ChG NADES measured over time, and (h) in water and 50% ChG NADES at 20 °C and 37 °C.

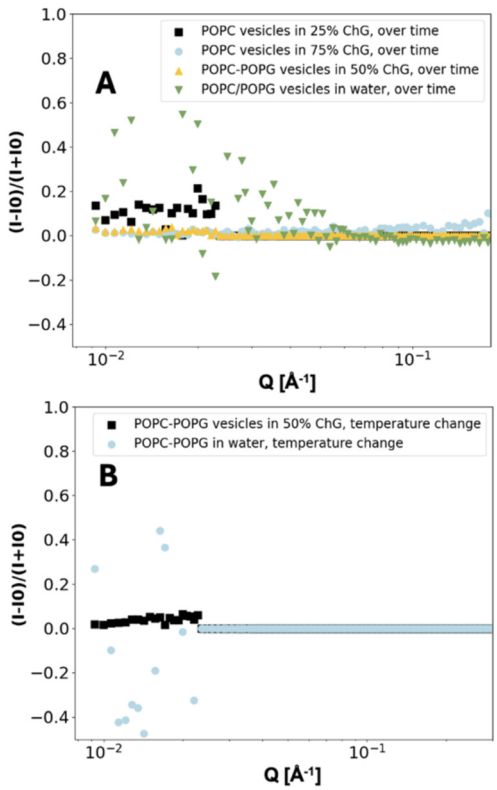

Fig. 8 (A) Difference in scattering intensity at 1 hour and 11 hour for POPC vesicles in 25% and 75% ChG, and (B) POPC–POPG vesicles in 50% ChG.

in agreement with the protective effect seen in the past for protein structure against temperature induced denaturation at similar NADES concentrations.[29] The SAXS data suggest that the vesicles in NADES containing aqueous solutions are more stable against aggregation and subsequent sedimentation than those made in pure water. The reason is not clear at this point, but one may speculate that changes in the hydrogen bonding structure and hydration layers may affect the vesicle–vesicle interactions.

Conclusions

In this work, we show that lipid vesicles made of pure POPC or in mixtures with POPG can be prepared in highly concentrated aqueous solutions of natural deep eutectic solvents both of neutral and acidic nature. The vesicles were analysed by dynamic light scattering and small angle X-ray scattering to determine their sizes and their structure in terms of lipid volume, lipid tail and head thicknesses, interfacial roughness, degree of multi-lamellarity and interbilayer distance. The vesicles were compared to those prepared in saline (NaCl) solutions matching the NADES osmolarity used hereby. The main results indicate that the lipid vesicle structure is maintained in NADES rich aqueous solutions even at high concentrations (75 wt%) and that the vesicle structure is protected against the high osmolarity or high saline conditions since no significant changes in bilayer structure occur in the presence of NADES as compared to pure water, but major changes take place in high saline conditions. Thus, the presence of NADES in water solutions have indeed a protective role in terms of maintaining the lipid bilayer structure.

Author contributions

Marité Cárdenas: conceptualization, writing – original draft preparation, formal analysis, investigation, methodology, visualization, supervision, funding acquisition. Victoria Ariel Bjørnestad: investigation, data curation, formal analysis, resources, reviewing and editing. Kari Kristine Almåsvold

Borgos: investigation, formal analysis, resources, reviewing and editing. Reidar Lund: conceptualization, formal analysis, writing – reviewing and editing, supervision, methodology, funding acquisition.

Data availability

Data are available upon request from the authors.

Conflicts of interest

There are no conflicts to declare.

Acknowledgements

The authors thank the Hanseatic League of Science (HALOS) project supported by EU Interreg Öresund-Kattegat-Skagerrak. M. C. thanks the Swedish Research Council (2022-03322, 2018-04833 and 2018-03990) for funding. RL is grateful to the Norwegian Research Council (NFR/RCN) for Grant No. 315666. This publication is part of project number PID2022-137440NB-I00, funded by MCIN/AEI/10.13039/501100011033/FEDER, UE. We also greatly acknowedge support by RECX – the Norwegian Resource Centre for X-rays funded by the Norwegian Research Council (208896).

References

1 D. Rente, M. Cvjetko Bubalo, M. Panić, A. Paiva, B. Caprin, I. Radojčić Redovniković and A. R. C. Duarte, Review of deep eutectic systems from laboratory to industry, taking the application in the cosmetics industry as an example, *J. Cleaner Prod.*, 2022, **380**, 135147.
2 S. Beil, M. Markiewicz, C. S. Pereira, P. Stepnowski, J. Thöming and S. Stolte, Toward the Proactive Design of Sustainable Chemicals: Ionic Liquids as a Prime Example, *Chem. Rev.*, 2021, **121**, 13132–13173.
3 Y. H. Choi, J. van Spronsen, Y. Dai, M. Verberne, F. Hollmann, I. W. C. E. Arends, G.-J. Witkamp and R. Verpoorte, Are natural deep eutectic solvents the missing link in understanding cellular metabolism and physiology?, *Plant Physiol.*, 2011, **156**, 1701–1705.
4 M. Bystrzanowska, F. Pena-Pereira, Ł. Marcinkowski and M. Tobiszewski, How green are ionic liquids? – A multi-criteria decision analysis approach, *Ecotoxicol. Environ. Saf.*, 2019, **174**, 455–458.
5 A. Benedetto, Ionic liquids meet lipid bilayers: a state-of-the-art review, *Biophys. Rev.*, 2023, **15**, 1909–1939.
6 Y. Dai, E. M. Varypataki, E. A. Golovina, W. Jiskoot, G.-J. Witkamp, Y. H. Choi and R. Verpoorte, in *Advances in Botanical Research*, ed. R. Verpoorte, G.-J. Witkamp and Y. H. Choi, Academic Press, 2021, vol. 97, pp. 159–184.
7 A. Sanchez-Fernandez and A. J. Jackson, in *Advances in Botanical Research*, ed. R. Verpoorte, G.-J. Witkamp and Y. H. Choi, Academic Press, 2021, vol. 97, pp. 69–94.
8 C. Knudsen, K. Bavishi, K. M. Viborg, D. P. Drew, H. T. Simonsen, M. S. Motawia, B. L. Møller and T. Laursen, Stabilization of dhurrin biosynthetic enzymes from Sorghum bicolor using a natural deep eutectic solvent, *Phytochemistry*, 2020, **170**, 112214.
9 M. Atilhan, L. T. Costa and S. Aparicio, On the behaviour of aqueous solutions of deep eutectic solvents at lipid biomembranes, *J. Mol. Liq.*, 2017, **247**, 116–125.
10 J. H. Crowe, J. F. Carpenter and L. M. Crowe, The role of vitrification in anhydrobiosis, *Annu. Rev. Physiol.*, 1998, **60**, 73–103.
11 H. L. Nystedt, K. G. Grønlien and H. H. Tønnesen, Interactions of natural deep eutectic solvents (NADES) with artificial and natural membranes, *J. Mol. Liq.*, 2021, **328**, 115452.
12 M. Tang, A. J. Waring and M. Hong, Trehalose-protected lipid membranes for determining membrane protein structure and insertion, *J. Magn. Reson.*, 2007, **184**, 222–227.
13 Q. Qiao, J. Shi and Q. Shao, Effects of water on the solvation and structure of lipase in deep eutectic solvents containing a protein destabilizer and stabilizer, *Phys. Chem. Chem. Phys.*, 2021, **23**, 23372–23379.
14 USPTO, *US Pat.*, 4927637, 1990.
15 D. G. Hunter and B. J. Frisken, Effect of extrusion pressure and lipid properties on the size and polydispersity of lipid vesicles, *Biophys. J.*, 1998, **74**, 2996–3002.
16 F. Nallet, R. Laversanne and D. Roux, Modelling X-ray or neutron scattering spectra of lyotropic lamellar phases: interplay between form and structure factors, *J. Phys. II*, 1993, **3**, 487–502.
17 M. A. Kiselev, P. Lesieur, A. M. Kisselev, D. Lombardo and V. L. Aksenov, Model of separated form factors for unilamellar vesicles, *Appl. Phys. A: Mater. Sci. Process.*, 2002, **74**, s1654–s1656.
18 P. Heftberger, B. Kollmitzer, F. A. Heberle, J. Pan, M. Rappolt, H. Amenitsch, N. Kučerka, J. Katsaras and G. Pabst, Global small-angle X-ray scattering data analysis for multilamellar vesicles: the evolution of the scattering density profile model, *J. Appl. Crystallogr.*, 2014, **47**, 173–180.
19 P. V. Konarev, A. Y. Gruzinov, H. D. T. Mertens and D. I. Svergun, Restoring structural parameters of lipid mixtures from small-angle X-ray scattering data, *J. Appl. Crystallogr.*, 2021, **54**, 169–179.
20 H. Frielinghaus, Small-angle scattering model for multilamellar vesicles, *Phys. Rev. E:Stat., Nonlinear, Soft Matter Phys.*, 2007, **76**, 051603.
21 V. Pipich, *QtiSAS: user-friendly program for reduction, visualization, analysis and fit of SA(N)S data*, 2020.
22 H. A. Faizi, S. L. Frey, J. Steinkühler, R. Dimova and P. M. Vlahovska, Bending rigidity of charged lipid bilayer membranes, *Soft Matter*, 2019, **15**, 6006–6013.
23 V. Nele, M. N. Holme, U. Kauscher, M. R. Thomas, J. J. Doutch and M. M. Stevens, Effect of Formulation Method, Lipid Composition, and PEGylation on Vesicle Lamellarity: A Small-Angle Neutron Scattering Study, *Langmuir*, 2019, **35**, 6064–6074.

24 P. Kumari, A. Faraone, E. G. Kelley and A. Benedetto, Stiffening Effect of the [Bmim][Cl] Ionic Liquid on the Bending Dynamics of DMPC Lipid Vesicles, *J. Phys. Chem. B*, 2021, **125**, 7241–7250.
25 D. Marsh, Molecular volumes of phospholipids and glycolipids in membranes, *Chem. Phys. Lipids*, 2010, **163**, 667–677.
26 H. L. Scott, A. Skinkle, E. G. Kelley, M. N. Waxham, I. Levental and F. A. Heberle, On the Mechanism of Bilayer Separation by Extrusion, or Why Your LUVs Are Not Really Unilamellar, *Biophys. J.*, 2019, **117**, 1381–1386.
27 N. Kučerka, M.-P. Nieh and J. Katsaras, Fluid phase lipid areas and bilayer thicknesses of commonly used phosphatidylcholines as a function of temperature, *Biochim. Biophys. Acta, Biomembr.*, 2011, **1808**, 2761–2771.
28 J. Cornier, A. Owen, A. Kwade and M. Van de Voorde, Nanoparticle Characterization Methods: Applications of Synchrotron and Neutron Radiation, in *Pharmaceutical Nanotechnology: Innovation and Production*, ed. J. Cornier, A. Owen, A. Kwade and M. Van de Voorde, 2017, DOI: **10.1002/9783527800681**.
29 N. F. Gajardo-Parra, L. Meneses, A. R. C. Duarte, A. Paiva and C. Held, Assessing the Influence of Betaine-Based Natural Deep Eutectic Systems on Horseradish Peroxidase, *ACS Sustainable Chem. Eng.*, 2022, **10**, 12873–12881.

